A NEW LOOK AT NOISE IN TRANSFERRED ELECTRON OSCILLATORS

Hans R. Gnerlich, John Ondria
Lehigh University
Packard Laboratory, Building 19
Electrical Engineering Department
Bethlehem, PA 18015

Abstract

Low frequency current and voltage fluctuations have been measured, and it has been confirmed that noise in packaged Transferred Electron Devices (TEDs) is due to three distinct noise mechanisms: Flicker, generation-recombination, and thermal noise. For Transferred Electron Oscillators (TEOs), this low frequency noise is upconverted into the microwave frequency range and adds to the intrinsic RF noise. We have found that, between 1 kHz and 1 MHz off the carrier, temperature dependent generation-recombination noise is the main contributor to the total noise. An improved model of a noisy TEO is presented. This model permits the calculation of AM and FM noise spectra from device and circuit parameters for measured low frequency noise or the derivation of device characteristics from noise and circuit parameter measurements.

Introduction

Acket[1], Copeland[2], DeCacquerary et al[3], and many others have shown that generation-recombination noise is a major contributor to the low frequency noise of bulk n-GaAs. Sweet[4] found that AM and FM noise is due to intrinsic (RF) noise, thermal in origin, and "excess noise", a low frequency noise that is upconverted into the microwave range and has a 1/f characteristic. What happened to the generation-recombination noise? The purpose of this investigation is to study the AM and FM noise characteristic of TEOs and identify the physical causes of noise from the measured data. To verify the experimental findings, a simplified model of a nonlinear oscillator is discussed, describing the noise behavior of the TEO in steady state oscillations.

Measuring System

The experimental work has been performed on n-type GaAs TEDs mounted in waveguide cavities. All TEDs and cavities are commercially available.

The noise measuring system is shown in Fig. 1. A comparative method is used to measure low frequency TEO noise below and above threshold, cf., Fig. 1b. The semiconductor is replaced by an equivalent reference resistor to eliminate the need of knowing quantitatively measuring system noise figure and gain. The AM-FM noise measuring system, described in detail by Ondria[5], is shown in principle in Fig. 1c. A noisy signal is demodulated in the balanced mixer. The AM components of the noise sidebands are obtained using path 1 as a direct detection system while path 2 is terminated. The FM components, converted to AM in path 2, are combined in the balanced mixer with the re-introduced 90 degree phase shifted carrier of path 1.

Low Frequency Noise of TEOs

The low frequency noise current of TEOs is measured below and above threshold and compared with theoretical spectra of bulk semiconductors.

The mean square noise currents of a TEO, biased above and below threshold, are compared in Fig. 2. The noise caused by trapping centers is dominant. Due to the increase of sample temperature, approximately 100°K above heatsink temperature for the TEO biased above threshold, the contribution of generation-recombination has been shifted from low to high frequencies.

The variation of low frequency noise with temperature is shown in Fig. 3 for a TEO biased above threshold. The portions of the spectrum due to generation-recombination noise are temperature sensitive, whereas, 1/f noise is temperature independent. In most cases, we found that cooling of a TEO increased noise in a frequency range approximately 1 kHz to 100 kHz. We were able to identify three separate noise mechanisms in the frequency range 20 Hz to 18 MHz: (a) flicker noise for frequencies below 10 kHz, (b) generation-recombination noise between 1 kHz and 10 MHz, and (c) thermal noise above 1 MHz.

Using the theoretical mean square noise current in bulk semiconductors and curve fitting techniques, the time constants τ associated with generation-recombination noise were determined. For example, we obtained values of τ at 300°K to be approximately 4 ms (15 ms for other devices) and $2 \leq \tau \leq 4\mu s$.

AM and FM Noise in TEOs

Measured AM and FM noise of TEOs mounted in waveguide cavities is compared with the low frequency noise of these devices.

For a modulating frequency range, 20 Hz < f_m < 18 MHz, the correlation between low frequency noise current $\sqrt{\overline{i_G^2}}$ and frequency deviation Δf_{rms} is shown in Fig. 4. A smooth curve drawn through the measured points follows approximately a straight line from 20 Hz to 1 MHz, described by

$$\Delta f_{rms} = M_{FI} f_{10} Q_L^{-1} \sqrt{\overline{i_G^2}} \,. \qquad (1)$$

For known RF frequency f_{10} and loaded quality factor Q_L, the frequency modulation sensitivity due to current fluctuations M_{FI} can be determined from the graph. Where Δf_{rms} is independent of low frequency current fluctuations, FM noise is only due to intrinsic (RF) noise. From this value of Δf_{rms}, equivalent noise temperature[6] T_n can be estimated. (For all devices measured we found $8 < M_{FI} < 19$ and $7{,}000°K < T_n$ $26{,}000°K$).

Low frequency noise current $\sqrt{i_G^2}$ produces bias voltage fluctuations $\sqrt{v_G^2}$ across the low frequency admittance. Adding parallel conductances changes the voltage fluctuations, cf. Fig. 5, and, therefore, the upconverted noise, cf. Fig. 6. Correlation of low frequency voltage fluctuations and FM noise are shown in Fig. 7, for R = 25 Ω and R = 1,500 Ω. For the greater value of R, upconverted noise dominates and intrinsic (RF) noise cannot be detected.

An increase of bias resistance increases the amount of bias fluctuations, cf. Fig. 5, and, therefore, AM noise, cf. Fig. 8. Correlation between AM noise and low frequency noise voltage is shown in Fig. 9. For large input impedance, the amount of upconverted noise is much larger than intrinsic noise. AM and low frequency noise are proportional. (The change in slope of the R = 25 Ω curve is not understood at this time.)

An Equivalent Circuit for TEOs

To verify our experimental findings, a simplified model[7,8] of a nonlinear oscillator is discussed, describing the noise behavior of the TEO in steady state oscillations. Since the active part of a TED is usually small compared to its wavelength in free space, a current-voltage equivalent circuit for the fundamental frequency of oscillation is defined at the active device terminals. The TED, cf. Fig. 10, is represented by admittance $\vec{Y}_D$, free of intrinsic noise, in parallel with noise current generator $\vec{I}_n$. The circuit and load admittance $\vec{Y}_C$ is transformed by the diode package to the TED terminals.

The condition for stable oscillations is

$$\vec{I}_n + \vec{V}_1[\vec{Y}_D(V_0,I_1) + \vec{Y}_C(f_1)] = 0, \qquad (2)$$

where V_0 is the bias voltage, I_1, V_1 and f_1 are RF current, voltage and frequency, respectively. Substituting magnitude and phase angle, defined in Fig. 10, (2) can be solved for the RF variations

$$\Delta I_1 = \frac{\frac{\partial \Delta Y_D}{\partial V}\sin(\theta_V-\theta_C)\Delta V_0 + \frac{Y_D}{I_{10}}\sin(\theta_n+\theta_D-\theta_C)I_n}{\frac{\partial \Delta Y_D}{\partial I}\sin(\theta_I-\theta_C)}, \qquad (3)$$

$$\Delta f_1 = \frac{\frac{\partial \Delta Y_D}{\partial V}\sin(\theta_I-\theta_V)\Delta V_0 + \frac{Y_D}{I_{10}}\sin(\theta_I-\theta_n-\theta_D)I_n}{\frac{d\Delta Y_C}{df}\sin(\theta_I-\theta_C)}, \qquad (4)$$

which are linear functions of low frequency variations ΔV_0 and RF noise $I_n(t)$. Referred to double sidebands, noise to carrier power ratio

$$\frac{P_{AM}}{P_1} = B[M_A^2\Delta V_0^2(f_m) + T_A^2 I_n^2(f_m)], \qquad (5)$$

and rms frequency derivation

$$\Delta f_{rms} = \frac{f_0}{Q_L}[B(M_F^2\Delta V_0^2(f_m) + T_F^2 I_n^2(f_m))]^{1/2}. \qquad (6)$$

can be calculated[8] from the spectral densities of ΔI_1 and Δf_1. Amplitude modulation sensitivity

$$M_A = \frac{\partial \Delta Y_D}{\partial V}\sin(\theta_V-\theta_C)\, I_{10}\frac{\partial \Delta Y_D}{\partial I}\sin(\theta_I-\theta_C)^{-1}, \qquad (7)$$

the transformation coefficient of RF noise current to AM noise power

$$T_A = Y_D\left[I_{10}^2\frac{\partial \Delta Y_D}{\partial I}\sin(\theta_I-\theta_C)\right]^{-1}, \qquad (8)$$

loaded oscillator quality factor

$$Q_L = f_{10}\frac{d\Delta Y_C}{df}\sin(\theta_I-\theta_C)\{2\,\mathrm{Re}[Y_C(f_{10})]\}^{-1}, \qquad (9)$$

frequency modulation sensitivity

$$M_F = \frac{\partial \Delta Y_D}{\partial V}\sin(\theta_I-\theta_V)\{\sqrt{2}\,\mathrm{Re}[Y_C(f_{10})]\}^{-1}, \qquad (10)$$

and transformation coefficient of RF noise current to rms deviation

$$T_F = Y_D\{\sqrt{2}\,I_{10}\,\mathrm{Re}[Y_C(f_{10})]\}^{-1}. \qquad (11)$$

Since AM and FM noise have the same origin, a cross spectrum $\overline{\Delta I_1 \Delta f_1}$ results. The cross-correlation coefficient was evaluated from case to case.

Equations (5) and (6) verify our experimental findings, cf. Figs. 4, 7, 9. Close to the carrier, AM and FM noise is proportional to low frequency noise which itself is proportional to bias resistance.

Conclusions

(a) Generation-recombination noise contributes to the total noise of TEOs between approximately 1 kHz and 1 MHz off the carrier. We have identified the impurities causing the trapping centers of this noise. Control of the impurities during manufacturing will reduce the total noise. (b) Measurements of low-frequency noise, less costly than RF-noise measurements, give an indication of AM and FM noise spectra to be expected. (c) The improved model of a noisy TEO permits calculation of AM and FM noise spectra from device parameters for known measured low frequency noise. (d) Circuit and/or device parameters can be calculated from measurements of low frequency and RF noise.

Acknowledgements

The authors wish to thank the U.S. Army Research Office, Durham for their support under Grant DA-ARO-D-31-124-71-G41.

References

1. G. A. Acket, "Recombination and Trapping in Epitaxial N-type Gallium Arsenide", Phillips Research Reports 26, pp. 261-278, 1971.

2. J. A. Copeland, "Semiconductor Impurity Analysis from Low Frequency Noise Spectra", IEEE Trans. ED-18, pp. 50-53, Jan. 1971.

3. A. DeCacqueray, G. Glasquez, J. Graffeuil, "Etude du Bruit de Generation Recombination de Diodes Gunn", Solid State Electronics, V 16, pp. 853-860, Aug. 1973.

4. A. A. Sweet, L. A. MacKenzie, "FM Noise in CW Gunn Oscillators", Proc. IEEE, May 1970.

5. J. G. Ondria, "A Microwave System for Measurement of AM and FM Noise Spectra", IEEE MTT-16, pp 767-781, Sept. 1968.

6. A. Ataman, W. Harth, "Intrinsic FM Noise of Gunn Oscillators", IEEE Trans. ED-20, pp. 12-14, Jan. 1973.

7. M. S. Gupta, "Noise Characteristics of Avalanche Transit Time Microwave Diodes", Dissertation, University of Michigan, 1972.

8. H. R. Gnerlich, "Noise in Transferred Electron Oscillators", Dissertation, Lehigh University, 1975.

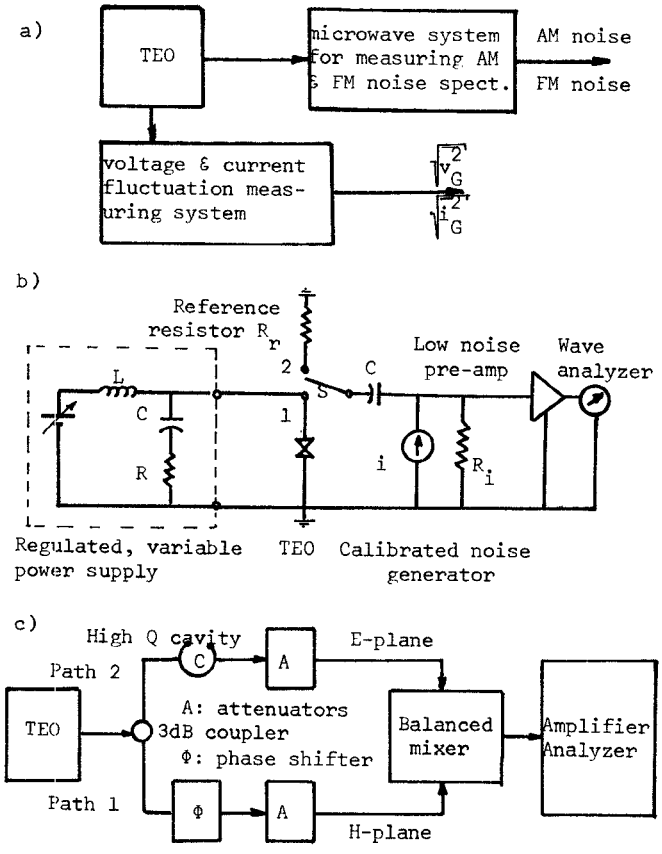

Fig.1. Noise measuring system. a) Principle of measurement, b) low frequency and c) microwave set-up.

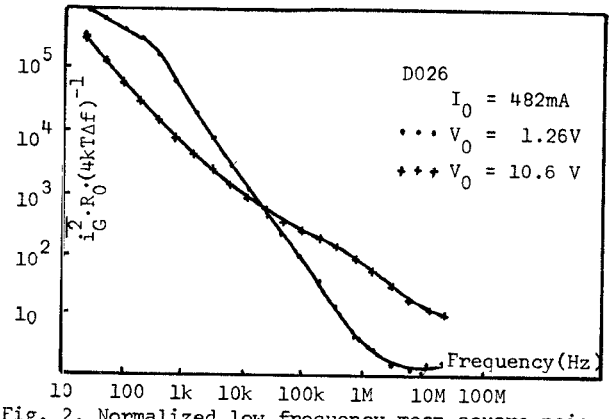

Fig. 2. Normalized low frequency mean square noise current below and above threshold vs frequency.

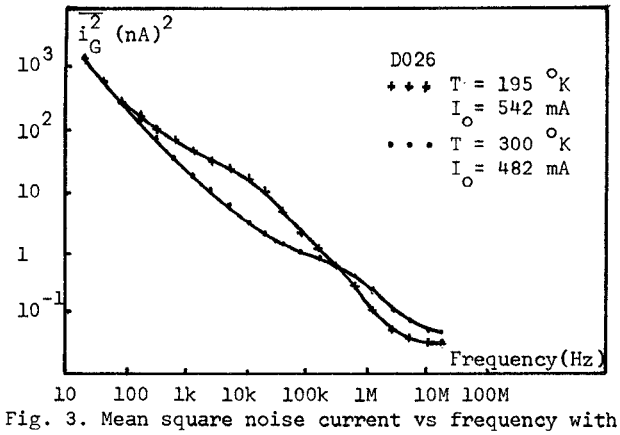

Fig. 3. Mean square noise current vs frequency with temperature as parameter.

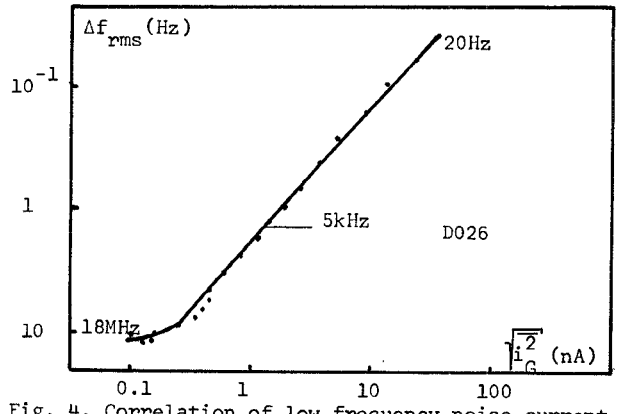

Fig. 4. Correlation of low frequency noise current and frequency deviation per unit bandwidth. Frequency is parameter and increases from right to left.

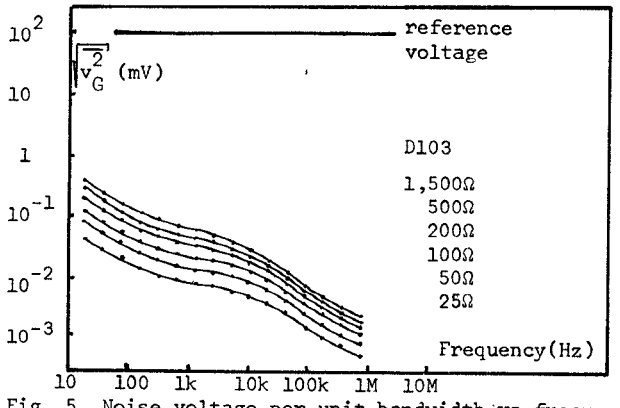

Fig. 5. Noise voltage per unit bandwidth vs frequency. Bias resistance parameter.

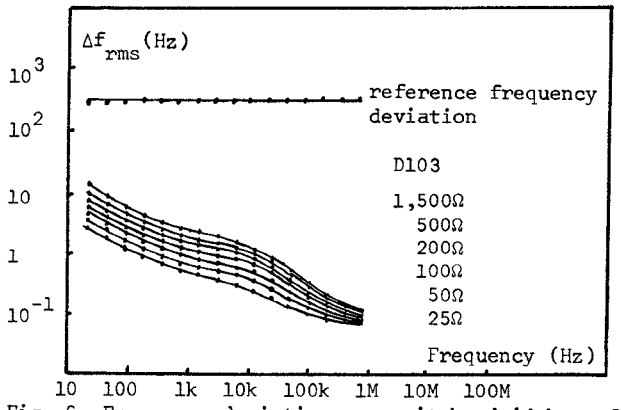

Fig. 6. Frequency deviation per unit bandwidth vs frequency. Bias resistance is parameter.

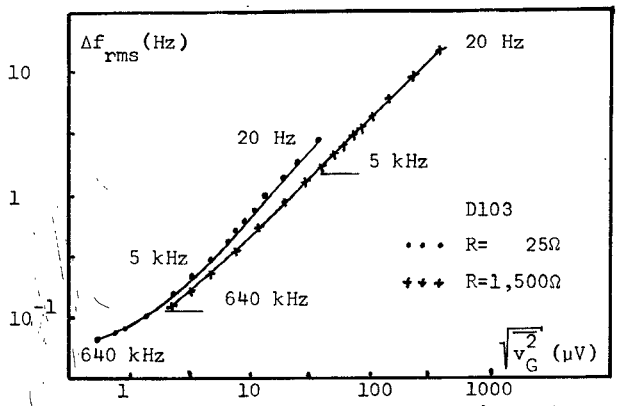

Fig. 7. Correlation of low frequency noise voltage and frequency deviation, per unit bandwidth. Frequency is parameter and increases from right to left.

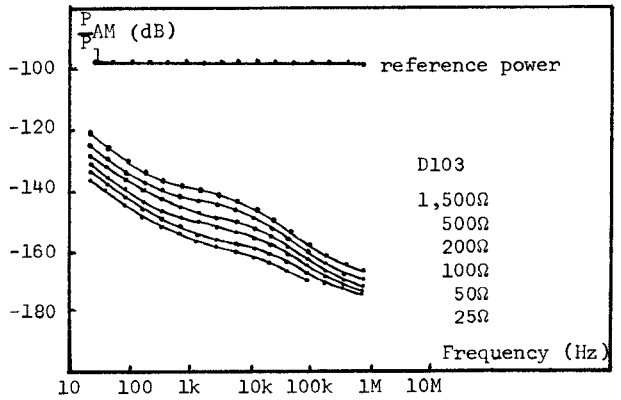

Fig. 8. AM noise spectrum per unit bandwidth vs frequency. Bias resistance is parameter.

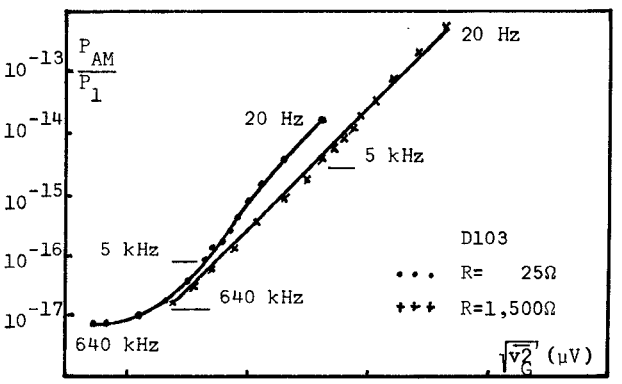

Fig. 9. Correlation of low frequency noise voltage and AM noise power. Frequency is parameter and increases from right to left.

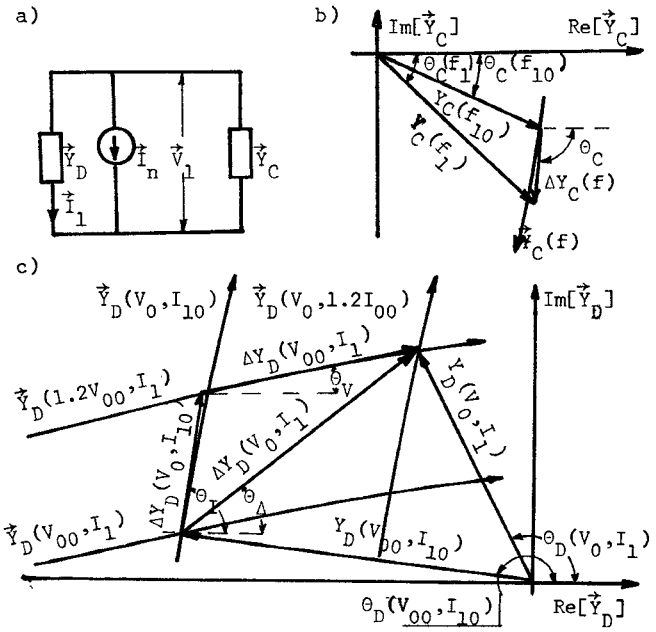

Fig. 10. TEO. a) Model of TEO at fundamental frequency f_1, b) circuit admittance as function of RF frequency, c) TED admittance as function of RF current and bias voltage.